Study on Preparation of Heterogeneous Polysulfone Affinity Filter Membrane and Its Sorption Properties for Hg^{2+}

Bing Wang, Yongfang Cui, Qiyun Du, Guangling Pei

School of Material Science and Chemical Engineering, Tianjin Polytechnic University, Tianjin 300160, China

Received 17 October 2001; accepted 28 March 2002

ABSTRACT: High quality heterogeneous polysulfone affinity flat filter membranes having chelating groups were prepared by phase separation by the use of blends of chelating resin and polysulfone as membrane materials, *N*,*N*-dimethylacetamide as the solvent, and water as the extraction solvent. The effects of blending ratio, chelating resin grain size, and temperature of casting solution on the structure of affinity membranes were investigated. The sorption process of an affinity filter membrane for Hg^{2+}, adsorbed under various chelating conditions such as chelating resin grain size, pH value, and the concentration of the metallic ion solution, was also studied. The results revealed that the greatest chelating capacity of an affinity filter membrane for Hg^{2+} was 1050 $\mu g/cm^2$ per membrane under appropriate conditions, and the sorption isotherms of Hg^{2+}could be expressed by the Freundlich sorption model. Dynamic chelating experiments indicated that the Hg^{2+} could be extracted with the affinity filter membrane and reextracted under acidic conditions. © 2002 Wiley Periodicals, Inc. J Appl Polym Sci 87: 908–915, 2003

Key words: resins; polysulfone; membranes; extraction/reextraction; chromatography

INTRODUCTION

Affinity filter membranes integrate the advantages of both affinity chromatography and modern membrane techniques.[1–6] The affinity filter membrane with definite millipores has an affinity agent on its inner and outer surface as a carrier of the affinity agent. When fluid is filtered through the membrane, the object products will quickly combine with the relevant functional groups of the affinity agent. The products sorbed on the membrane will soon be desorbed when an eluent passes through the membrane. Consequently, the separate period is short and the coefficient of affinity functional groups' use is substantial. In addition, because the membrane has good properties of fluid traversing, mechanical stability, and low operating pressure of the equipment, the process engineering is apt to be magnified. Metal mercury (Hg), inorganic mercury salt, and organic mercury compounds can negatively affect a person's health.[7] After inhalation into the human body, mercury vapor can easily accumulate in the central nervous system, liver, and kidney. In the bloodstream, the mercury ion can firmly combine with protein in nephrocytes, thus causing destruction of kidney function. Organic mercury compounds [e.g., methyl mercury $(CH_3)_2Hg$] are apt to dissolve in fat and accumulate in the human body.

Poisonous mercury-containing industrial effluents, which come from the plants that use or produce mercury and mercury compounds, are the major source of mercury pollution. It is reported that manufacturers used thiocarbamide and iminodiacetic acid as chelating agents in ion-exchange membranes for the removal of mercury, and the chelating capacity of the two kinds of membranes for Hg^{2+} were 600 $\mu g/cm^2$ per membrane and 92 mg/g per membrane, respectively.[8,9] Amidophosphoric acid resin, prepared by styrene–divinylbenzene copolymer by chloromethylation, ammoniation, and phosphorylation, is a kind of chelating resin. It can selectively chelate metal ions by ionic bond and covalent bond.[10] In this study, amidophosphoric acid resin was used as a carrier of chelating affinity agent and blended with polysulfone, to prepare a new type of heterogeneous chelating affinity filter membrane for the removal of Hg^{2+}, and the maximum chelating capacity of Hg^{2+} could reach 1050 $\mu g/cm^2$ per membrane.

EXPERIMENTAL

Preparation of chelating affinity filter membrane

Affinity filter membranes were prepared by the phase inversion method.[11] The amidophosphoric acid resin (APAR) used in this study was supplied by Nankai University Chemical Plant (China). Polysulfone (PSF)

Correspondence to: B. Wang (hxl_009@sina.com).

Journal of Applied Polymer Science, Vol. 87, 908–915 (2003)

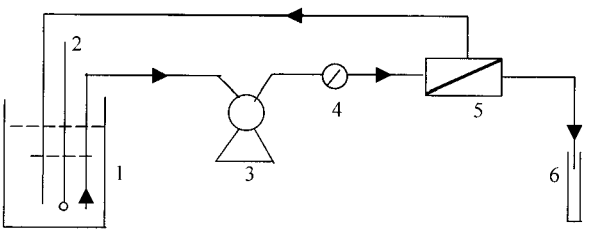

Figure 1 Schematic diagram of the water flux measurement apparatus of a flat membrane. 1: reservoir; 2: centigrade thermometer; 3: water pump; 4: pressure meter; 5: flat membrane module; 6: volumetric cylinder.

was obtained from Shanghai Shuguang Chemical Plant (China). *N*,*N*′-Dimethylacetamide (DMAc) was obtained from Tianjin Chemical Reagent Plant (China). The APAR/PSF composites were prepared by the physical blending method and used as membrane materials. An amount of PSF was dissolved in DMAc to form a certain concentration of PSF solution. Then the quantitative APAR that was ground and sifted was put into the PSF solution and the solution of APAR/PSF was rigorously stirred for 7 h. Because the APAR could not be dissolved in DMAc, the solution of APAR/PSF was heterogeneous. A certain composition of heterogeneous APAR/PSF casting solution could be obtained after vacuum deaeration. The heterogeneous casting solution was cast onto a glass pane and coagulated in water at 30°C to form a smooth APAR/PSF membrane. The membranes were preserved in a wet state to prevent pores of the membrane from contracting.

Observation by SEM

In the previous work, we dipped the sample of membrane in 50% glycerol, after which it was removed and air-dried; the glycerol on its surface was removed, and the sample was broken off after being frozen in liquid nitrogen. The microstructure of both the surface and a cross section of the membrane was observed with an S450 scanning electron microscope (Hitachi, Japan).

Water flux measurement

The schematic diagram of experimental apparatus for measurement of water flux is shown in Figure 1. In this apparatus (Tianjin Polytechnic University, China), the ultrapure water circulated from the feed reservoir of 2000 mL volume, through a water pump, through the module, and back into the feed reservoir. Other ultrapure water that was filtered through the membrane was received in the volumetric cylinder. The pressure was 0.1 MPa, and the medium was ultrapure water. From the measured volume V of transmission liquid and filtration time t, the water flux Q was calculated by the following relationship:

$$Q = \frac{V}{At} \tag{1}$$

where A is the effective surface area of the membrane.

Porosity measurement

The porosity of the membrane (P_r) was determined by means of the gravimetry method.[12] We used glycerol as saturant, sheared a definite area of wet membrane, wiped off the glycerol on the surface of the membrane, and weighed the wet membrane (W_w). The wet membrane was then moved into a vacuum dry box to dry until its weight was unchanged. Finally, we weighed the dry membrane (W_d). The porosity of the membrane P_r was calculated from eq. (2), as follows:

$$P_r = \frac{W_w - W_d}{Sd\rho} \times 100\% \tag{2}$$

where S is the superficial area of the wet membrane, d is the average thickness of the membrane, and ρ is the density of glycerol.

Membrane pore size measurement

The membrane pore size was determined by means of the filtering velocity method.[12] The membrane pore diameter r_f was calculated from eq. (3):

$$r_f = \sqrt{\frac{8 \times (2.90 - 1.75P_r)\mu LQ}{P_r \Delta PA}} \tag{3}$$

where P_r is porosity, L is the thickness of the membrane, μ is the viscosity of the transmission liquid, Q is the flux, ΔP is the pressure, and A is the filtering area.

Sorption property of the affinity filter measurement

We dipped the piece of membrane into $Hg(NO_3)_2$ (analytical reagent; Tianjin Chemical Reagent Plant) solution and determined the sorption amount of the membrane for Hg^{2+} after a definite time. The chelating sorption amount Γ was calculated from eq. (4) as follows:

$$\Gamma = (C_0 - C_t)/S \tag{4}$$

where C_0 is the original content of Hg^{2+} when the membrane was not dipped into the immersion solution, C_t is the residual content of Hg^{2+} when the membrane was dipped into the immersion solution, and S is the membrane area.

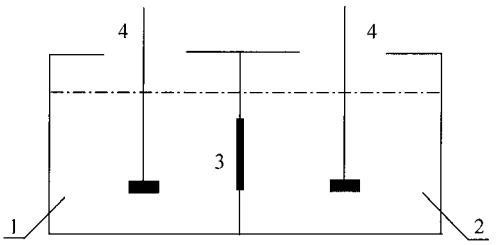

Figure 2 Schematic diagram of dynamic sorption experiment of the affinity membrane for Hg^{2+}. 1: $Hg(NO_3)_2$ solution; 2: HNO_3 solution; 3: affinity membrane; 4: agitator.

Hg^{2+} quantity measurement

Hg^{2+} analyses were carried out by use of the dithizone method.[13] In acid medium, Hg^{2+} reacted upon an overdose of dithizone to form orange-yellow dithizonate $Hg(HDz)_2$ that could be dissolved in CCl_4. The free dithizone was removed with dilute NH_3 solution. At wavelength λ_{max} = 485 nm, the extinction of $Hg(HDz)_2$ solution was determined with a Model 7220 spectrophotometer (Beijing RuiLi Instrument Plant, China). Further, the Hg^{2+} quantity associated with $Hg(HDz)_2$ extinction could be determined.

Dynamic chelating sorption properties of the membrane measurement

A schematic diagram of the dynamic chelating sorption experimental system is shown in Figure 2. It was self-made and composed of two vessels. One was full of $Hg(NO_3)_2$ solution and the other was full of HNO_3 solution. An affinity membrane was fixed between the two vessels. The change of Hg^{2+} concentration in the two vessels was determined with respective reaction times.

RESULTS AND DISCUSSION

SEM of the membrane with different contents of chelating resin

Figure 3 and Figure 4 are scanning electron micrographs, respectively, of the cross section and surface of the membranes with different contents of chelating resin. From the figures, it can be seen that the cross section of the membrane is divided into two parts: one is a dense layer, the other a loose layer. In the loose layer, the pores of the membrane were tiny and well distributed. Generally, they were vertical and nonpenetrating finger-shape pores. The pores in the dense layer were smaller and well distributed. However, the pores in the loose layer surface were comparatively larger and not well distributed. The APAR/PSF casting solution was cast onto a glass pane and coagulated in water at a certain temperature to form a flat membrane. When the casting solution on the glass pane coagulated in water, the gel speed of PSF macromolecules was fast on the casting solution upper superficial layer, the time of precipitation and coagulation of PSF macromolecules was short, and a large number of PSF macromolecules could not gather at once. Before

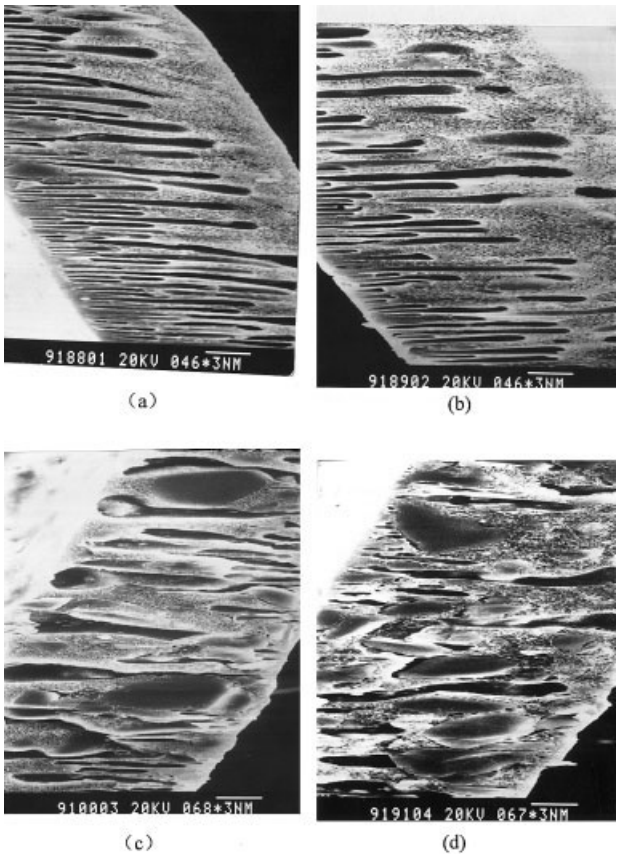

Figure 3 Scanning electron micrographs of cross section of affinity membrane made by phase inversion method at various chelating resin contents: (a) 10%; (b) 30%; (c) 55%; (d) 65%.

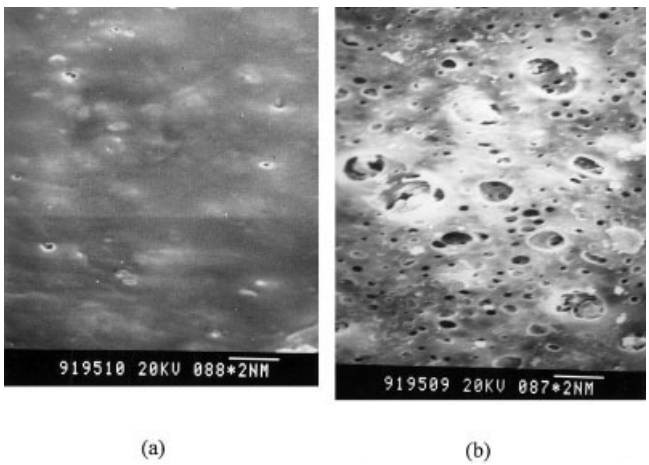

Figure 4 Scanning electron micrographs of surface of affinity membrane made by phase inversion method: (a) dense layer; (b) loose layer.

TABLE I
Effect of Chelating Resin Content on the Properties of Chelating Filter Membranes[a]

Resin content (%)	Water flux ($mL/cm^{-2}/h^{-1}$)	Pore diameter (nm)	Porosity (%)
0	0.40	4.7	89.3
10	0.38	5.1	88.1
20	6.00	22.0	75.3
30	18.01	27.1	71.0
55	24.01	51.0	70.1
65	24.00	52.7	64.0

[a] Chelating resin pore diameter 4.0–5.0 nm; chelating resin grain diameter 97–105 μm; casting solution temperature 30°C.

coagulation, the obvious two phases were hardly able to form. Thus the dense layer formed on the casting solution upper superficial layer and severely blocked the diffusion exchange of DMAc with water. Because of the coagulation velocity decrease, the PSF macromolecules had enough time to form larger block masses. After the PSF block masses coagulated and the DMAc diffused, the separation among the block masses formed larger nanopores. The nanopores in the loose layer were larger than those in the dense layer. From the figures, it can also be seen that, compared with the finger-shape pores of the membrane with content 10% chelating resin, the pores of the membrane with content 55–65% chelating resin were obviously large, and the number of the pores was decreased. The chelating resin grains could be well distributed in the PSF solution when the content of chelating resin was lower. Thus when PSF formed a concentrated phase, the interference of chelating resin was negligible. With the increase of chelating resin content, the interference of chelating resin increased, the diffusion speed of coagulant decreased, and the coagulation speed of PSF macromolecules in the loose layer decreased. It gave rise to a lesser degree of loose layer and pores of the membrane increased.

Effect of chelating resin content on the structure of the membrane

Changes in the structure of the membrane with chelating resin content are shown in Table I. From Table I it can be seen that in the range of 10%, the water flux and pore size were less, the porosity was greater, and the effect of chelating resin content on the structure of membrane was negligible. In the low concentration region the content of chelating resin was less. Thus in the process of phase inversion the membrane pores appeared mainly in the continuous phase of PSF. First, the PSF macromolecules gathered together, formed the concentrated phase, and became an island structure. The parts among the islands formed the dilute phase. With the solvent (DMAc) diffusion, the concentration phase formed the dense parts of the membrane and the dilute phase formed the pores of the membrane. The size of the pores could be controlled by the speed of the phase inversion. The pore diameter of membrane changed suddenly from several nanometers to tens of nanometers when the content of chelating resin increased to 20%. This means that the mechanism of pore formation changed. Chelating resin and PSF formed a heterogeneous membrane, and had partial compatibility. With the increase of the content of chelating resin, the degree of phase separation increased, and the nanopore diameters increased among the chelating resin phases and PSF phases. When the content of chelating resin was greater than 20%, the trend of gathering of chelating resin macromolecules could be enhanced, the phases separated to a significant degree, and the nanopore diameters between the two phases were increased; thus the water flux also increased with them. However, the number of nanopores decreased in unit volume and the porosity decreased, too.

Effect of size of chelating resin grains on the structure of the membrane

Figure 5 shows scanning electron micrographs of the cross section of membranes with different sizes of chelating resin grains and additionally shows that pores of the membrane underwent an obvious change with different sizes of chelating resin grains. When the diameter of chelating resin grains was 97–105 μm, the membrane pores were the largest; when the diameter of chelating resin grains was 125–147 μm, the pores of membrane were larger; and when the diameter of chelating resin grains was 74–88 μm, the membrane pores were normal. Table II shows the changes in the structure of the membrane with different sizes of chelating resin grain. From Table II it can be seen that with decreasing size of chelating resin grains, the water flux and pore size increased first and then decreased later. This was related to the interface sorption between chelating resin and casting solution. Chelating resin grains simultaneously adsorbed PSF and DMAc. With the decrease in size of chelating resin grains and the increase of interface energy, the adhesion increased between chelating resin and PSF solution, and the size of the interface pores decreased. With the diffusion of solvent (DMAc), the macromolecules had greater opportunity to gather and form more colloid network structures when the membrane was prepared by the phase inversion method. Thus the ratio of the larger gathering pores and porosity of membrane increased. Meanwhile, the degree of both connections increased with the decrease in size of the chelating resin grains. When the PSF macromolecules assembled in the coagulation bath, they drove the

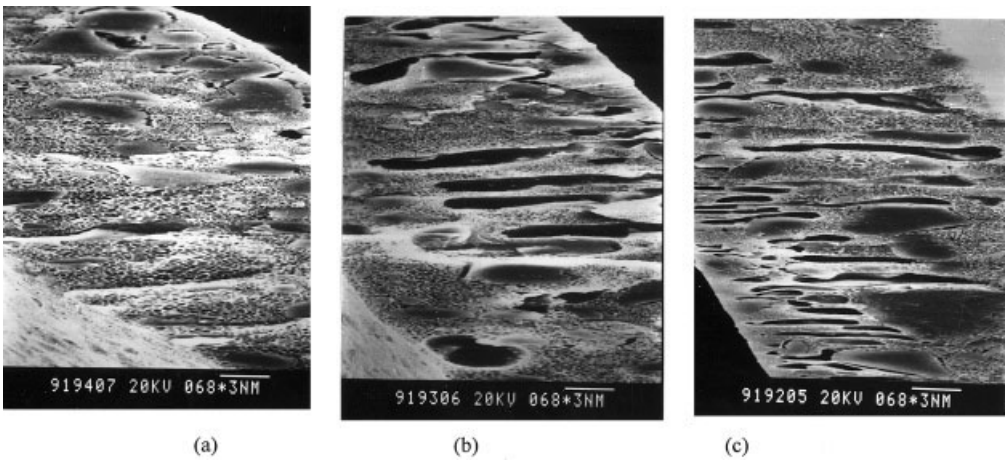

Figure 5 Scanning electron micrographs of cross section of affinity membrane made by phase inversion method of varying chelating resin grain diameters: (a) 74–88 μm; (b) 97–105 μm; (c) 125–147 μm.

chelating resin grains to move, forming larger pores and increasing water flux.

Effect of temperature of casting solution on the structure of the membrane

Changes in the structure of the membrane with temperature of casting solution are shown in Table III. Table III shows that water flux, size of pores, and porosity of membrane all decreased with the increase of temperature of the casting solution. The reason was that, as the viscosity of casting solution decreased, the solvent (DMAc) molecules were much more easily diffused in the coagulation bath, the water molecules around the piece of membrane were affected by heat sent from the membrane, and the water molecules diffused more quickly with the increase of temperature. Because the elimination speed of the solvent was high, almost all the PSF macromolecules had insufficient time to gather before gelatification, and many compact tiny pores had been formed.

Effect of chelating resin grain size on the sorption amount of the membrane for Hg^{2+}

Figure 6 shows changes in the sorption amount of Hg^{2+} with sorption time for membrane with different sizes of chelating resin grain. From Figure 6 it can be seen that there is a sharp increase in the sorption of Hg^{2+} with the increase of sorption time until a time of 13 h was reached, beyond which the sorption tended to reach a plateau (remaining almost constant regardless of the time increase) for different chelating resin grain diameters. During the initial stage of the sorption reaction, there were many chelating functional groups on the membrane pores and the speed of sorption reaction of Hg^{2+} was very fast. With the increase of sorption time, the sorption amount of Hg^{2+} increased rapidly. When the sorption time reached 13 h, the chelating functional groups had been reacted completely, the sorption had been saturated, and the sorption amount no longer changed with time. From Figure 6 it can also be seen that during the reaction initial stage, the three absorption isotherms of Hg^{2+} did not coincide, which indicates that the chelating resin grain size produced an effect on the sorption amount of Hg^{2+}. The smaller the chelating resin grain size, the greater the specific surface of chelating resin. It also means that both sorption speed and saturated absorption amount of Hg^{2+} increased with the decrease of chelating resin grain size.

TABLE II
Effect of Chelating Resin Grain Diameter on the Properties of Chelating Filter Membranes[a]

Grain diameter (μm)	Water flux (mL/cm^{-2}/h^{-1})	Pore diameter (nm)	Porosity (%)
125–147	11.31	17.1	72.91
97–105	17.46	26.5	62.29
74–88	3.18	9.5	65.85

[a] Chelating resin pore diameter 4.0–5.0 nm; chelating resin grain content 30%; casting solution temperature 25°C.

TABLE III
Effect of Temperature of the Casting Solution on the Properties of Chelating Filter Membrane[a]

Temperature (°C)	Water flux (mL/cm^{-2}/h^{-1})	Pore diameter (nm)	Porosity (%)
25	12.61	40.2	62.3
30	8.73	38.8	36.5
40	3.31	30.3	34.8
50	2.50	14.4	33.2

[a] Chelating resin pore diameter 4.0–5.0 nm; chelating resin grain diameter 125–147 μm; chelating resin grain content 30%.

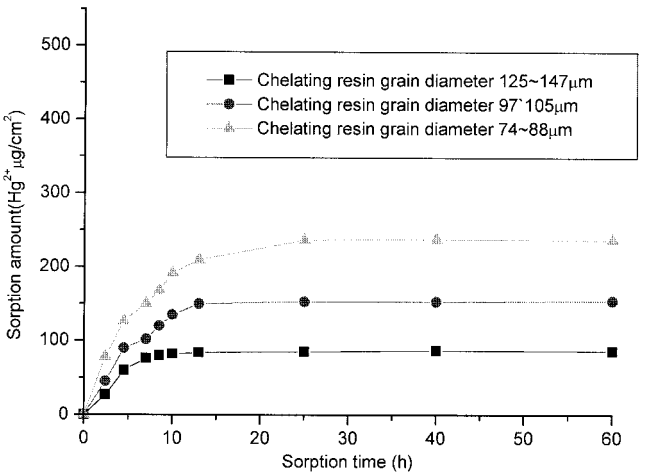

Figure 6 Effect of chelating resin size on the sorption amount of membrane. Chelating resin content, 20%; pH = 7.

Effect of salinity on the sorption amount of the membrane for Hg^{2+}

Changes in the sorption amount of Hg^{2+} with sorption time for membrane in different salinity solutions are shown in Figure 7. From Figure 7 it can be seen that both sorption speed and sorption capacity of the membrane for Hg^{2+} were increased with the increase of Hg^{2+} concentration. Hg^{2+} conducted ionic exchange with H^+ on the affinity filter membrane. According to the membrane theory of Donnan,[14] the ionic-exchange balance is affected by the electrolytic concentration and ionic valence state. In the initial stage of the reaction, the speed of exchange sorption increased with the increase of Hg^{2+} concentration. During the process of the reaction, the concentration gradient was formed around the membrane and the ionic potential difference was also formed. Because of the push of ionic potential difference, Hg^{2+} could be adsorbed continuously with the membrane. When the ionic potential difference of the inner and outer portions of the membrane reached balance, the sorption amount of Hg^{2+} could no longer change. Figure 8 shows that the logarithm of chelating capacity Γ and Hg^{2+} concentration C was mainly in conformity with the Freundlich empirical equation[15] at 22°C:

$$\log \Gamma = n \log C + K$$

Effect of salt solution pH on the chelating sorption amount of membrane for Hg^{2+}

Figure 9 shows changes in the sorption amount of Hg^{2+} with sorption time for membranes in solutions of different pH values. From Figure 9 it can be seen that in the range of pH = 1.2–3.0, sorption speed and sorption capacity of the membrane for Hg^{2+} increased with the increase of pH. Sorption isotherms of Hg^{2+} were close in the range of pH = 3.0–4.0. The functional group of chelating resin in the membrane was $-CH_2$-NH-CH_2-PO(OH)$_2$. The Hg^{2+} not only displaced the H of the P-OH group, but also coordinated the lone electron of the amidogen N atom into chelate. When the pH was lower, amidogen combined with H^+ to form salt. It meant that the lone electron could not coordinate with Hg^{2+}, and the chelating sorption of membrane for Hg^{2+} was restrained. It can also be seen from Figure 9 that the sorption of Hg^{2+} could reach an adsorption equilibrium after 3.2 h in the range of pH = 1.2–2.0; the sorption of Hg^{2+} could reach an adsorption equilibrium after 6.2 h in the range of pH = 3.0–4.0. The saturated absorption amount of Hg^{2+} increased with the increase of pH value. In fact, the pH value of the solution could not be increased infinitely; otherwise, the Hg^{2+}combined with OH^- to form a precipitant, and the membrane could not be used for removal of Hg^{2+} from the solution. The elution of membrane was opposite to the sorption of the membrane. The elution amount of Hg^{2+} was negligible when the pH value of eluent was greater than 3.0. The elution amount of Hg^{2+} was greater and the elution speed was very fast when the pH value of the eluent was lower than 1.2.

Dynamic chelating process of the membrane for Hg^{2+}

In the dynamic sorption experimental system, $Hg(NO_3)_2$ solution and pure water or HNO_3 solution were positioned beside the affinity filter membrane. Figure 10 shows the change of Hg^{2+} concentration with chelating sorption time. The Hg^{2+} concentration in the pure water vessel was slight and hardly changed with sorption time, and the Hg^{2+} concentration in the $Hg(NO_3)_2$ solution vessel decreased quickly with the increase of sorption time. The reason was that

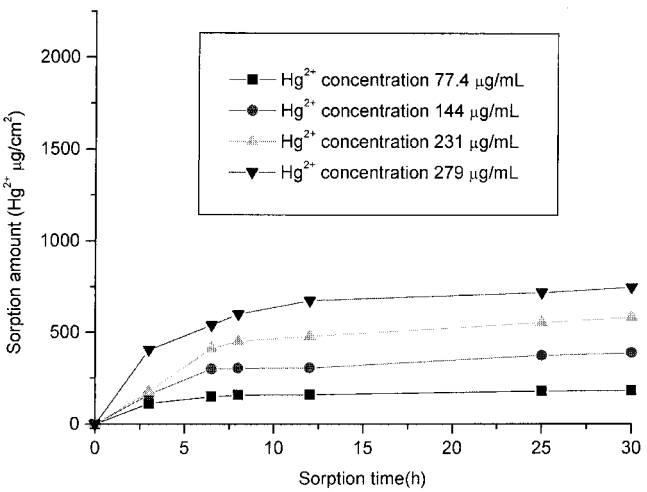

Figure 7 Effect of Hg^{2+} concentration on the sorption amount of membrane. Chelating resin content, 20%; chelating resin grain diameter, 97–105 μm; pH = 7.

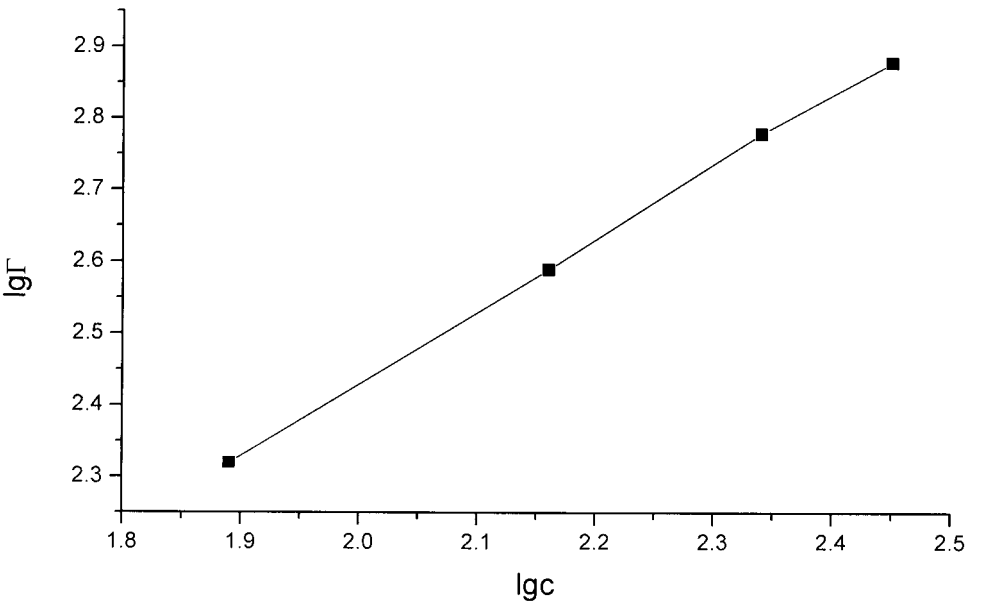

Figure 8 Relationship of Hg^{2+} concentration and sorption amount of membrane. Chelating resin content, 20%; chelating resin grain diameter, 97–105 μm.

in the diffusion process the Hg^{2+} was captured and adsorbed by the affinity filter membrane. Figure 11 shows the change of Hg^{2+} concentration with sorption time in two vessels. There was an affinity filter membrane between the two vessels. The $Hg(NO_3)_2$ solution was put into the left vessel, and the HNO_3 solution was put into the right vessel. It could be found that the Hg^{2+} concentration in the $Hg(NO_3)_2$ solution vessel (left vessel) decreased with sorption time, and Hg^{2+} concentration in the HNO_3 solution vessel (right vessel) increased with sorption time. Passing through the affinity filter membrane, the Hg^{2+} was adsorbed. Meanwhile, the Hg^{2+} that had been adsorbed on the membrane was displaced by the H^+. As discussed above, sorption and desorption of Hg^{2+}could be realized simultaneously.

CONCLUSIONS

Our investigation proved that the blends of APAR/PSF can be used to prepare high quality heterogeneous affinity filter membranes with high chelating capacity for Hg^{2+}. Several processing parameters, such as mass ratio of chelating resin to PSF in the casting solution, the temperature of casting solution, and the chelating resin grain size, had obvious effects on the structure of the membrane. The sorption rate

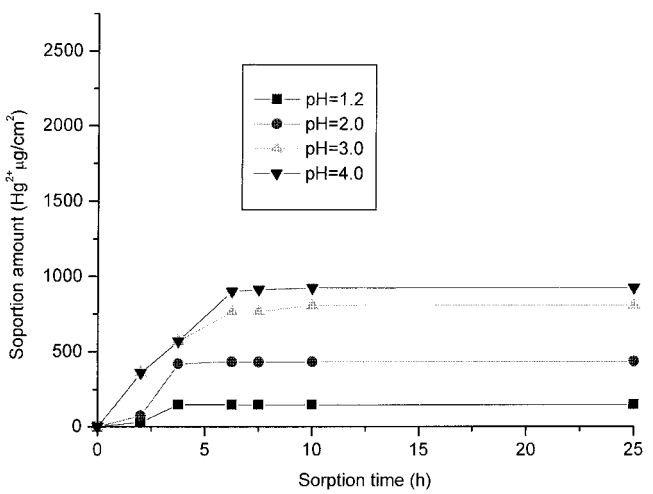

Figure 9 Effect of pH on the sorption of membrane. Chelating resin content, 20%; chelating resin grain diameter, 90–105 μm; pH = 7.

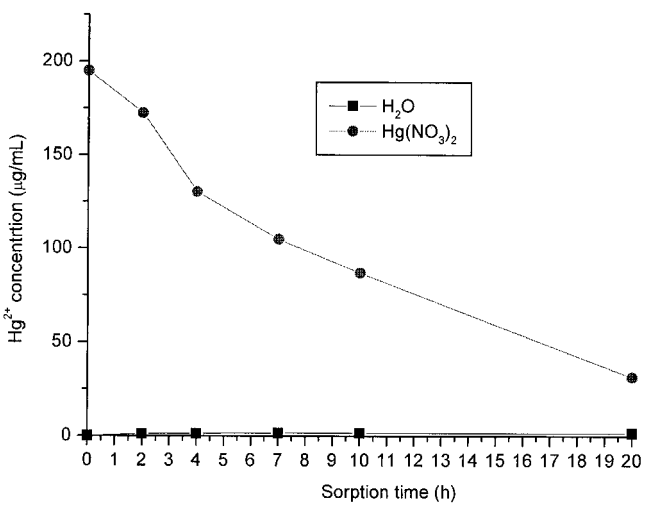

Figure 10 Relationship between Hg^{2+}concentration and sorption time. Chelating resin content, 20%; chelating resin grain diameter, 90–105 μm; pH = 7.

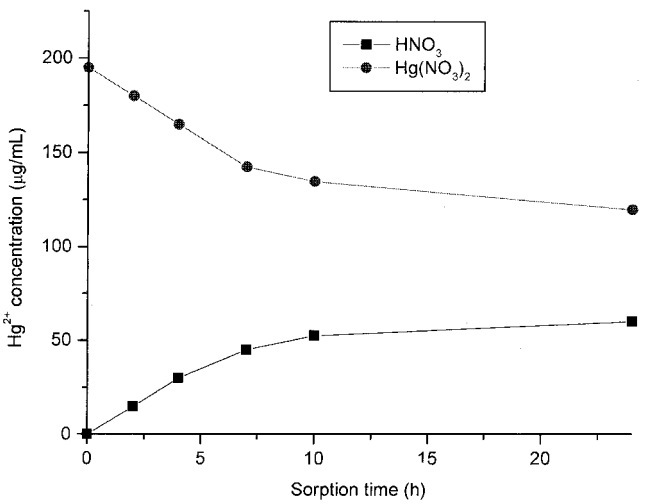

Figure 11 Relationship between Hg^{2+}concentration and sorption time. Chelating resin content, 20%; chelating resin grain diameter, 90–105 μm; 1 mol/L HNO_3.

and sorption capacity of the membranes for Hg^{2+} could be affected by the chelating reaction conditions and average grain size of chelating resin. Extraction and reextraction of Hg^{2+}could be carried out in the course of the dynamic mass transfer process. Compared with other chelating membranes for removal of Hg^{2+}, the heterogeneous polysulfone affinity filter membrane had a greater chelating capacity for Hg^{2+}. The affinity filter membrane could be used to retrieve Hg^{2+} in the mercury-containing industrial effluent.

References

1. Beeskow, T. C.; Kusharyoto, K.; Anspach, F. B. J Chromatogr A 1995, 715, 49.
2. Serfica, G. C.; Pimbley, J.; Belfort, G. J Membr Sci 1994, 88, 292.
3. Reif, O. W.;Volker, N.; Bahr, U. J Chromatogr A 1993, 654, 29.
4. Petsch, D.; Beeskow, T. C.; Anspach, F. B. J Chromatogr B 1997, 693, 79.
5. Li, J.; Chen, H.; Chai, H. Chem J Chin Univ 1999, 20, 1322.
6. Bao, S.; Shi, G.; Jiang, W. J Chem Ind Eng (China) 1995, 46, 15.
7. Dai, S. Environmental Chemistry; Higher Education Press: Beijing, 1997; pp 299–305.
8. Guo, Z.; Du, Q.; Deng, X. Technol Water Treat (China) 1988, 14, 8.
9. Wang, Z. Ion Exchange Membrane; Chemical Industry Press: Beijing, 1986; p 128.
10. Zhang, Z.; Qian, T.; Xu, G. Ion Exchange Adsorp 1988, 4, 42.
11. Osada,Y.; Nakagawa, T. Membrane Science and Technology; Marcel Dekker: New York, 1992; p 8.
12. Gao, Y.; Ye, L. Membrane Separation Technology Base; Science Press: Beijing, 1989; p 173.
13. Dranitskaya, R. M.; Gavrilchenko, A. I.; Okhitina, L. A. Zh Analit Khim 1970, 25, 1740.
14. Osada, Y.; Nakagawa, T. Membrane Science and Technology; Marcel Dekker: New York, 1992; pp 26–29.
15. Osada, Y.; Nakagawa, T. Membrane Science and Technology; Marcel Dekker: New York, 1992; pp 36–38.